

# 1 How local interactions impact the dynamics of an 2 epidemic

3 Lydia Wren, Alex Best

4 *School of Mathematics and Statistics, University of Sheffield, Sheffield, S3 7RH, UK*

---

## 5 Abstract

Susceptible-Infected-Recovered (SIR) models have long formed the basis for exploring epidemiological dynamics in a range of contexts, including infectious disease spread in human populations. Classic SIR models take a mean-field assumption, such that a susceptible individual has an equal chance of catching the disease from any infected individual in the population. In reality, spatial and social structure will drive most instances of disease transmission. Here we explore the impacts of including spatial structure in a simple SIR model. In particular we assume individuals live on a square lattice and that contacts can be 'local' (neighbour-to-neighbour) or 'global' or a mix of the two. We combine an approximate mathematical model (using a pair approximation) and stochastic simulations to consider the impact of increasingly local interactions on the epidemic. We find that there is a strongly non-linear response, with small degrees of local interaction having little impact, but epidemics with substantially lower and later epidemics once interactions are predominantly local. We also show how intervention strategies to impose local interactions on a population must be introduced early if significant impacts are to be seen.

---

## 6 1. Introduction

7 The classic Susceptible-Infected-Recovered (SIR) model has long been used to  
8 model the spread of infectious disease in human, animal and plant populations  
9 (Kermack and McKendrick, 1927; Anderson and May, 1979). More recently it  
10 has formed a central pillar of much of the modelling of the Covid-19 pandemic

11 (Ferguson et al, 2020; Kucharski et al, 2020; Firth et al, 2020). In its standard  
12 form, the SIR model has a mean-field assumption, such that individuals in the  
13 population have purely random, ‘global’ interactions (Boots and Sasaki, 2000)  
14 and there is no spatial structure. In reality, individuals in a population are  
15 more likely to contract disease from infected individuals who are closer to  
16 them, both physically and socially. Incorporating this spatial structure into  
17 mathematical models is extremely challenging. In some cases, large datasets of  
18 known contact networks have been used to replicate epidemics to excellent  
19 effect (Ferguson et al, 2020; Firth et al, 2020). While such models have a high  
20 degree of realism and thus predictive power, they cannot be readily modelled  
21 by a simple set of equations and require significant computational exploration  
22 to capture possible outcomes and feedbacks.

23 One common approach to incorporating a degree of regular spatial structure,  
24 and particularly ‘local’ near-neighbour interactions, in to infectious disease  
25 models is to use a lattice-based probabilistic cellular automata (Sato et al,  
26 1994; Rand et al, 1995). These stochastic individual-based models have also  
27 been combined with an analytic pair-approximation method (Matsuda et al,  
28 1992; Sato et al, 1994), where the full spatial dynamics are approximated by a  
29 set of ordinary differential equations based on the classic SIR model. Such  
30 models have been applied to infectious disease systems both with (Keeling  
31 et al, 1997; Webb et al, 2007a,b; Best et al, 2012) and without (Keeling, 1999;  
32 Sharkey, 2008) demography. These have found that local interactions reduce  
33 the value of  $R_0$ , slowing or even preventing an epidemic that would occur  
34 when interactions are global (Keeling, 1999). These approaches largely insist  
35 on a strict degree of spatial structure, where infection and/or host  
36 reproduction can only be through near-neighbour interactions. While this is  
37 useful for comparison with the mean-field case, interactions are unlikely to be  
38 entirely local or global in reality, and we may be missing important features of  
39 systems where the interaction structure lies between these two extremes.

40 The ability to move between local, near-neighbour interactions and global,

41 mean-field interactions has been considered in a few spatial models of  
42 infectious disease, primarily in evolutionary (Boots and Sasaki, 1999, 2000;  
43 Kamo et al, 2007; Best et al, 2011; Débarre et al, 2012) and ecological (Ellner,  
44 2001; Webb et al, 2007a) contexts. This multiscale method is commonly  
45 achieved by allowing a proportion of transmission and/or reproduction to  
46 occur locally and the rest globally. We might interpret this, for example in a  
47 human population, as an individual mostly interacting within their household  
48 or community (local interactions), but also travelling some distance for work,  
49 holidays or visiting friends or family (global interactions). These studies have  
50 shown that there is increased potential for ecological cycles and disease-driven  
51 extinction as interactions become predominantly local (Webb et al, 2007a),  
52 while evolutionary selection is generally towards lower levels of infection in  
53 both host and parasite as interactions become more local (Boots and Sasaki,  
54 1999; Best et al, 2011), but not necessarily monotonically (Kamo et al, 2007).  
55 Most recently, this multiscale method has been applied to a human  
56 epidemiology model with equal births and deaths (Maltz and Fabricius, 2016),  
57 showing that pronounced (but damped) oscillations in infection may result  
58 after a sudden shift to local interactions. However, this simple mechanism to  
59 investigate the impacts of varying the degree spatial structure has yet to be  
60 applied to simple human epidemic models over short-term scales such that  
61 demography does not impact the dynamics.

62 In this study we present a combination of a stochastic individual-based model  
63 and a pair approximation of epidemics on a lattice. We explore how changing  
64 the proportion of local-to-global interactions alters the course of an epidemic  
65 and investigate whether increasing the degree of local interactions - which we  
66 may define as restrictions on movement - can lessen the impact of an epidemic.

## 67 **2. Model**

### 68 *2.1. Mean-field model*

69 The underlying dynamics of the model are based on the classic  
70 Susceptible-Infected-Recovered (SIR) epidemiological framework (Kermack

71 and McKendrick, 1927), with no demographic processes (births/deaths). We  
72 first consider the model under a mean-field assumption with no local  
73 interactions. All individuals in the population are either susceptible ( $S$ ),  
74 infected ( $I$ ) or recovered ( $R$ ). The total population size  $N = S + I + R$  is  
75 constant (assume  $N = 1$  for consistency with what follows), meaning we only  
76 need to track the dynamics of  $S$  and  $I$  densities, given by the following  
77 ordinary differential equations,

$$\begin{aligned}\frac{dS}{dt} &= -\beta SI \\ \frac{dI}{dt} &= \beta SI - \gamma I.\end{aligned}$$

78 Transmission is assumed to be density-dependent with coefficient  $\beta$ , while  
79 recovery occurs at rate  $\gamma$  and immunity is assumed to be permanent.

## 80 2.2. Pair-approximation model

81 To account for spatial structure and local transmission, we use a  
82 pair-approximation model (Matsuda et al, 1992). Assume individuals live on a  
83 square lattice, where each site is always occupied by one susceptible, infected  
84 or recovered individual. We define the probability that a site is occupied by a  
85 susceptible individual as  $P_S$ , an infected individual as  $P_I$  and a recovered  
86 individual as  $P_R$ . The dynamics of these 'singlet' densities mirror those of the  
87 mean-field model above, with the following ordinary differential equations,

$$\frac{dP_S}{dt} = -\beta [Lq_{S/I} + (1 - L)P_S] P_I \quad (1)$$

$$\frac{dP_I}{dt} = \beta [Lq_{S/I} + (1 - L)P_S] P_I - \gamma P_I \quad (2)$$

88 with  $P_R = 1 - P_S - P_I$ . Here we have introduced our key parameter,  $L$ , which  
89 determines the proportion of transmission that occurs 'locally' between  
90 neighbouring individuals, with the remainder of transmission  $(1 - L)$  occurring  
91 'globally' between random individuals on the lattice. This corresponds to  
92 individuals' interactions being predominantly local (with their near neighbours)

93 or global (randomly across the population). The conditional probability, called  
94 the 'environs density', that an infected individual has a neighbour that is  
95 susceptible is denoted  $q_{S/I} = P_{SI}/P_I$ . Therefore there are two routes to  
96 transmission:

- 97 • global:  $(1 - L)\beta P_S P_I$
- 98 • local:  $L\beta q_{S/I} P_I$ .

99 This system of equations is not closed, since to calculate the conditional  
100 probabilities we need to know the 'pair' density,  $P_{SI}$ , e.g. the probability that  
101 a randomly chosen pair of neighbouring sites are a susceptible and an infected.  
102 The dynamics of these pair densities are governed by an additional set of  
103 ordinary differential equations,

$$\frac{dP_{SS}}{dt} = -2\beta(L(3/4)q_{I/SS} + (1 - L)P_I)P_{SS} \quad (3)$$

$$\begin{aligned} \frac{dP_{SI}}{dt} &= -\beta(L((1/4) + (3/4)q_{I/SI}) + (1 - L)P_I)P_{SI} - \gamma P_{SI} \quad (4) \\ &+ \beta(L(3/4)q_{I/SS} + (1 - L)P_I)P_{SS} \end{aligned}$$

$$\frac{dP_{SR}}{dt} = -\beta(L(3/4)q_{I/SR} + (1 - L)P_I)P_{SR} + \gamma P_{SI} \quad (5)$$

$$\frac{dP_{II}}{dt} = -2\gamma P_{II} + 2\beta(L((1/4) + (3/4)q_{I/SI}) + (1 - L)P_I)P_{SI} \quad (6)$$

$$\frac{dP_{IR}}{dt} = -\gamma P_{IR} + \beta(L(3/4)q_{I/SR} + (1 - L)P_I)P_{SR} + \gamma P_{II}, \quad (7)$$

104 and  $P_{RR} = 1 - P_{SS} - P_{II} - 2P_{SI} - 2P_{SR} - 2P_{IR}$ . Again, this system of  
105 equations is not closed as we have further conditional probabilities that  
106 depend on 'triplets' (e.g.  $q_{I/SI} = P_{SII}/P_{SI}$ ). One can appreciate that this  
107 pattern will continue and that the equations will never form a closed system.  
108 We thus apply a 'pair approximation' (Matsuda et al, 1992) where we assume  
109 that, for example,  $q_{I/SI} = q_{I/S}$ , allowing us to close the system.

### 110 2.3. Basic reproductive ratio

111 The basic reproductive ratio,  $R_0$ , is the well-known quantity that measures the  
112 average number of secondary infections caused by an infected individual in an

113 otherwise disease-free population (Anderson and May, 1981). For the  
114 mean-field (global) case where  $L = 0$ , this is simply given by  $R_0 = \beta/\gamma$ . When  
115 interactions are fully local with  $L = 1$ , we have  $R_{0,l} = \beta q_{S/I}/\gamma$ . In the limit  
116 where the population is indeed entirely disease-free, the environs density  
117  $q_{S/I} = P_S = 1$ , and the two basic reproductive ratios will be equal. However,  
118 in the early stages of an epidemic the environs density  $q_{S/I}$  rapidly shrinks as  
119 the contact network is formed, meaning it quickly becomes that  $R_{0,l} < R_0$ ,  
120 leading to a slower epidemic (Matsuda et al, 1992; Keeling, 1999). Given the  
121 total reproductive ratio will be,

$$R_{0,t} = LR_{0,l} + (1 - L)R_0 \quad (8)$$

122 it is clear that the initial growth rate of an epidemic will be slower the greater  
123 the degree of local interactions.

#### 124 *2.4. Stochastic simulations*

125 Alongside these mathematical models we additionally conduct stochastic  
126 individual-based simulations using a probabilistic cellular automata. Similarly  
127 to the model described above, a lattice of sites is established, now of fixed size,  
128 where each site is again occupied by one individual. A Gillespie algorithm  
129 (Gillespie, 1977) is implemented for tau-leaping between events of recovery  
130 and transmission (local or global). At each step, exactly one of these events  
131 occurs, with probabilities proportional to their rates, and a suitable host is  
132 chosen randomly from the lattice for it to occur to (e.g. recovery requires an  
133 infected host to be selected). After an event occurs, the lattice is updated and  
134 a new tau-leap calculated for the next event. This approach is fully spatially  
135 explicit, unlike the approximation present in the mathematical methods above.  
136 Code for the models are provided as electronic supplementary material.

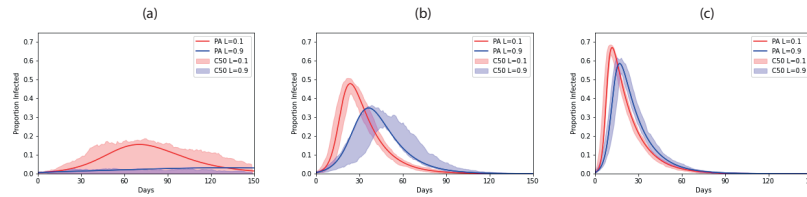


Figure 1: Epidemic curves from pair approximations and the ‘most central’ 50% of 100 stochastic simulations for different values of  $L$ .  $\gamma = 1/14$ . (a)  $R_0 = 2$ , (b)  $R_0 = 5$ , (c)  $R_0 = 10$ .

### 137 3. Results

#### 138 3.1. Epidemic curves

139 We begin by examining the epidemic curves predicted by the pair  
140 approximation and stochastic simulations for different values of  $L$  (0.1 and  
141 0.9) and different mean-field basic reproductive ratios,  $R_0$  (2, 5 and 10).

142 Recent work has highlighted the pitfalls of combining multiple stochastic  
143 individual-based models into simple static statistics of means and variances  
144 (Juul et al, 2020). We follow the methods of Juul et al (2020) by finding the  
145 ‘most central’ 50% of 100 simulated curves to present here (see appendix for  
146 details).

147 Focussing on the effect of increasing the proportion of local interactions, from  
148 figure 1 it is clear visually that the higher value of  $L$  produces a lower and  
149 later peak of infection. Restricting global interactions may therefore, in itself  
150 (without further reductions to transmission probability), slow down and limit  
151 the spread of an epidemic. Increasing  $R_0$  not only moves the epidemics earlier  
152 and higher, but also reduces the effect of local interactions. Comparing the  
153 plots, we can see that control mechanisms that both shift interactions from  
154 predominately global to predominately local *and* reduce  $R_0$  (for example,  
155 through both movement restrictions and ‘social distancing’ and hygiene  
156 measures) are predicted to have a significant effect on reducing the epidemic.

157 We can also compare the fit of the pair-approximation to the stochastic  
158 models. As we might expect, when  $L$  is small the pair approximation appears  
159 to present a reasonable ‘average’ of the stochastic model runs. As  $L$  becomes  
160 larger we find that, while the pair approximation often sits within the most  
161 central runs, for larger  $R_0$  at least, it tends to predict that the epidemic peak  
162 is rather earlier and higher than seen in most of the fully spatially-explicit  
163 model runs. The discrepancy between the pair approximation and stochastic  
164 simulations is most pronounced at low values of  $R_0$ . In particular, in this case  
165 a number of the stochastic simulations produce ‘failed’ epidemics, as evidenced  
166 by the lower bound of the 50% central curves running close to 0. In the online  
167 appendix we show that for  $L = 1$  and  $R_0 = 2$  around 30% of stochastic  
168 simulations do not result in an epidemic.

### 169 *3.2. Descriptive statistics*

170 We now explore the behaviour as we vary local interactions across the full  
171 range of  $L$  from 0 (fully global) to 1 (fully local). Five descriptive statistics  
172 were evaluated, with three presented here (percentage of the population  
173 infected by day 300, percentage of the population infected at the peak and the  
174 day of the peak) with two further statistics in the online appendix (days till  
175 less than 1% of the population were infected and days with greater than 15%  
176 of the population infected). In order to take results from the individual-based  
177 simulations, 100 runs of the model were created and the mean and variance of  
178 the aforementioned statistics were taken.

179 Two clear trends emerge from all of the results. Firstly, the impact of local  
180 interactions is significantly reduced the higher  $R_0$  is. For every statistic  
181 investigated, varying the value of  $L$  has little effect on the plots for  $R_0 = 10$ .  
182 Secondly, there is an accelerating impact of local interactions, with little effect  
183 seen as  $L$  is first increased from 0, but the impact growing as  $L$  moves towards  
184 1. Both effects are clear when plotting the percentage of the population  
185 infected by day 300 (broadly, the total infected during an epidemic in this  
186 case) in figure 2(a)-(c). When  $R_0 = 2$ , there is a slow decrease in the



It is made available under a [CC-BY-NC-ND 4.0 International license](https://creativecommons.org/licenses/by-nc-nd/4.0/) .

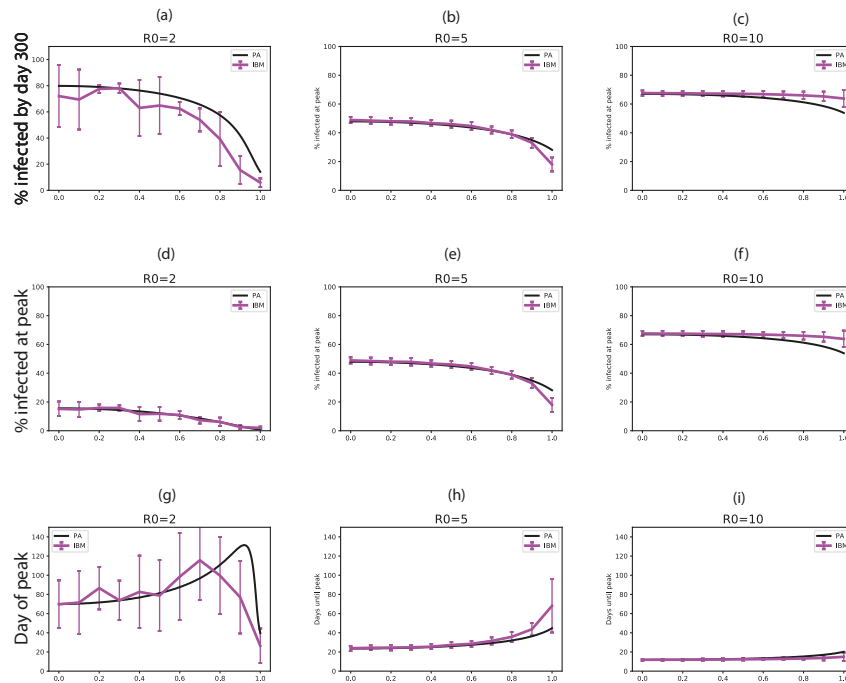


Figure 2: Descriptive statistics of PA and stochastic simulations. (a)-(c) Percentage of population infected by day 300. (d)-(f) Percentage infected at peak. (g)-(i) Day of peak.

187 percentage infected for  $0 < L < 0.6$ , but once  $L$  is greater than this there is a  
188 large accelerating decrease in the number of individuals infected during the  
189 epidemic. However for larger values of  $R_0$ , there is a smaller decrease which  
190 doesn't happen until  $L$  is almost 1. A similar pattern can be seen in plots  
191 (d)-(f): increasing  $L$  initially causes little change in the proportion infected at  
192 the peak of the epidemic, but then decreases more rapidly as  $L$  approaches 1,  
193 but this is less evident the higher  $R_0$  is.

194 Figure 2(g)-(i) shows that the number of days until the peak increases with  $L$ ,  
195 again accelerating as  $L$  increases. There is an exception to this when  $R_0 = 2$   
196 as  $L$  approaches 1. Here, the peak moves significantly earlier because the  
197 infection fails to spread through the population meaning the peak of the  
198 epidemic is both very early on and very low, as confirmed in figure 2a.  
199 Obviously, the larger  $R_0$  is, the faster the disease will be able to spread

200 through the population and therefore the faster it will die out (with no  
201 susceptible individuals left to infect).

202 In general, the pair approximation appears to be a good fit to the results from  
203 the stochastic model and is almost always within a standard deviation of the  
204 mean, but this fit appears to be least good as  $L$  approaches 1. The pair  
205 approximation is less accurate for  $R_0 = 2$  than for higher values of  $R_0$ , and  
206 this is likely due to the large proportion of infections which fail to become  
207 established in the stochastic model when the disease spreads slowly, resulting  
208 in a lower mean and larger standard deviation, as described in the online  
209 appendix.

### 210 *3.3. Using local interactions as a control mechanism*

211 We now explore how enforcing movement restrictions, resulting in more  
212 localised interactions, might impact the spread of an epidemic. We assume  
213 that initially a population has predominantly global interactions ( $L = 0.1$ ).  
214 We then assume that when a threshold of percentage infected (here, 5%) is  
215 reached, interactions immediately switch to being predominantly local  
216 ( $L = 0.9$ ) and remain so until the infected percentage returns below the  
217 threshold. Figure 3 shows that compared to the case where interactions  
218 remain predominantly global throughout (red), if movement restrictions are  
219 imposed (blue) the peak of the epidemic is reduced, but less substantially than  
220 if interactions had always been predmoniantly local, particularly for the lower  
221  $R_0$  (see figure 1 and table 1). Interestingly, we also see a second wave  
222 emerging for lower  $R_0$  once restrictions are lifted since the herd-immunity  
223 threshold has not been reached, suggesting further and/or longer restrictions  
224 may need to be imposed.

225 We further investigate by varying the threshold at which restrictions are  
226 imposed and the value of  $L$  moved to under the restrictions (figure 4).  
227 Changing the bound at which  $L$  increases seems to have relatively little effect  
228 on the course of the epidemic, with there being little change in the the number

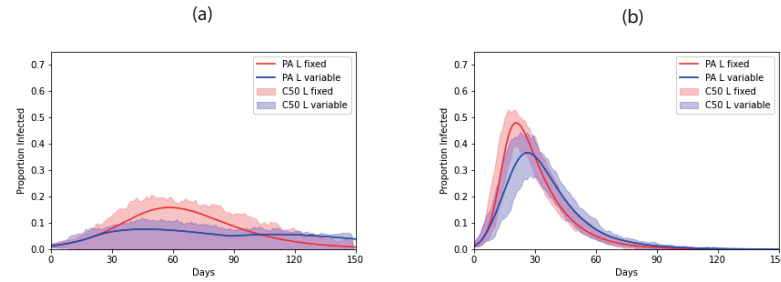


Figure 3: Epidemic curve with (a)  $R_0 = 2$  and (b)  $R_0 = 5$ . Red curves,  $L = 0.1$  throughout. Blue curves:  $L = 0.1$  until  $P_I > 0.05$ , then  $L = 0.9$  while  $P_I > 0.05$ , dropping back to  $L = 0.1$  thereafter.

Interaction	$R_0 = 2$	$R_0 = 5$
$L = 0.1$ constant	15.8%	48.0%
$L = 0.9$ constant	4.0%	35.3%
$L$ Varying	7.6%	36.6%

Table 1: Peak infections from PA for different levels of local interactions

229 of people infected, but a modest decrease in the peak and a somewhat later  
 230 peak for lower thresholds. When varying  $L$ , again there is little change in the  
 231 total proportion infected, a modest decrease in the peak for higher restrictions  
 232 but almost no change to the peak day. The variance in the results from the  
 233 stochastic simulations is large, suggesting that it may be more difficult to  
 234 predict the outcome of a disease once restrictions on global interactions are  
 235 implemented, but the mean of these results is close to the pair approximation.  
 236 When the higher  $L = 1$ , the PA results change dramatically, due to the  
 237 emergence of the second peak. As the higher  $L$  increases towards 0.9, it can be  
 238 seen that the impact of the epidemic is mitigated, with the biggest change  
 239 seen in the peak infected proportion of the population almost halving from  
 240  $L = 0.1$  to  $L = 0.9$ .

This relative lack of impact is because of the speed with which the lattice becomes correlated in the early stages of an epidemic. The correlation between

It is made available under a [CC-BY-NC-ND 4.0 International license](https://creativecommons.org/licenses/by-nc-nd/4.0/) .

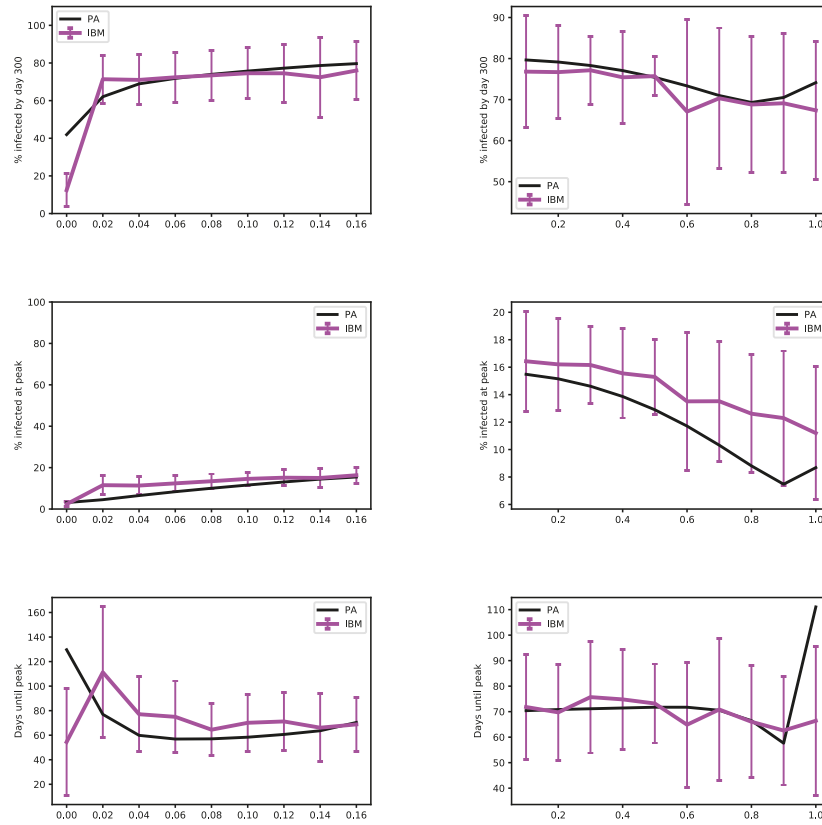


Figure 4: Impact of changing (a) the threshold at which interactions switch from  $L = 0.1$  to  $L = 0.9$  and (b) the degree of movement restrictions.

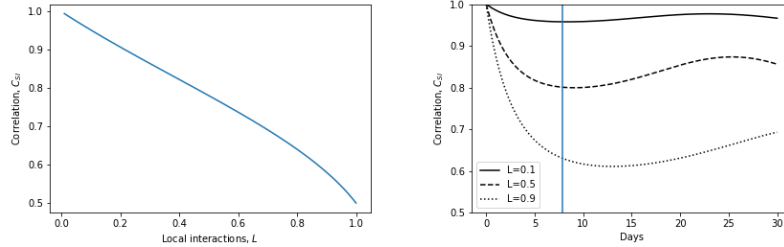


Figure 5: Correlation coefficient,  $C_{SI}$ , from pair approximation for different values of  $L$ . Left: Predicted quasi-equilibrium,  $\hat{C}_{SI}$  from equation (10). Right: Early-time correlation dynamics  $C_{SI}$  from full pair-approximation model. The vertical line marks where the quasi-equilibrium is reached when  $L = 0.1$ .

$S$  and  $I$  sites on the lattice is given by,

$$C_{SI} = \frac{P_{SI}}{P_S P_I} = \frac{q_{S/I}}{P_S}. \quad (9)$$

At the start of an epidemic with predominantly global interactions then the lattice is uncorrelated and  $C_{SI} = 1$ . During the early stages, the correlation rapidly approaches a quasi-equilibrium as the contact network forms (Keeling, 1999), which we show in the appendix can be approximated as,

$$\hat{C}_{SI} = \frac{3L - 2 + \sqrt{-7L^2 + 4L + 4}}{4L}. \quad (10)$$

241 Figure 5 shows that increasing  $L$  leads to much stronger early-time  $S$ - $I$   
 242 correlation, due to increasingly spatially-localised contact networks. If an  
 243 epidemic begins in a population with predominatly local interactions, the  
 244 lattice quickly becomes correlated,  $q_{S/I}$  falls and the infection slows itself  
 245 down due to a lack of locally available susceptible individuals. In contrast, if  
 246 an epidemic has established with predominatly global interactions, the  
 247 network is already highly uncorrelated before the movement restrictions are  
 248 imposed. The late implementation of local interactions therefore cannot cause  
 249 high correlation of the lattice, and a large number of local epidemics can still  
 250 occur.

#### 251 4. Discussion

252 In this study we have used a pair approximation alongside stochastic  
253 simulations to investigate the impact of local interactions on an epidemic. Our  
254 results show that epidemics where interactions are predominantly local will  
255 result in fewer infections spread over a longer period of time than those where  
256 interactions are global, in line with previous studies (Keeling, 1999).

257 Importantly, we find that the trends as we move from purely global to purely  
258 local interactions are not linear. Instead, our results consistently show initially  
259 flat responses in various infection statistics as  $L$  is increased, with rapid  
260 changes as  $L$  approaches 1. This suggests that the course of an epidemic in a  
261 population with relatively high proportions of local interactions (even 50:50)  
262 will be roughly the same as an epidemic in a population with purely global  
263 interactions. Even at relatively low proportions of global interactions, enough  
264 long-range infections can occur in the early stages of an epidemic to seed large  
265 numbers of local epidemics, allowing the infection to spread throughout the  
266 population. For example, if  $R_0 = 2$  and  $L = 0.5$ , on average an infected  
267 individual passes the disease to one local and one global contact, allowing the  
268 disease to become established across the lattice and to then form a series of  
269 outbreaks. It is only as  $L$  becomes close to 1 and almost all interactions are  
270 local that the likelihood that an infected individual transmits the disease  
271 globally is small enough to have a significant impact. Interestingly, in the  
272 similar model by Maltz and Fabricius (2016) that includes simple  
273 demographics (and thus yields an endemic equilibrium), the infected  
274 equilibrium is initially fairly static as interactions become more local before  
275 rapidly falling as local interactions become more dominant, suggesting this  
276 non-linear trend is robust in simple epidemic models.

277 Our results have important implications for attempting to limit an epidemic  
278 through restricting movement. In particular, such restrictions must be  
279 considerable, with almost all global interactions removed, if significant effects  
280 are to be seen. It is important to note that in our model restricting movement

281 does not lead to lowered per-individual contacts, as might be assumed under  
282 'lockdown' scenarios (for example due to social distancing, regular  
283 hand-washing, wearing masks, etc). We found that restrictions that both make  
284 interactions more local and infectious contacts less frequent (through lowered  
285  $R_0$ ) can substantially reduce the impact of an epidemic. Moreover, we found  
286 that if the population starts from a position of having predominantly global  
287 interactions, movement restrictions must be imposed very early on in the  
288 course of an epidemic or they will have minimal effect. This is due to the fact  
289 that, if a disease has already begun to spread randomly through a population  
290 with global contacts, when restrictions are put in place there will already be  
291 large numbers of local outbreaks forming across the lattice. If an infection has  
292 a particularly high  $R_0$ , and therefore rapid growth, it may be that infection is  
293 already too widespread for movement restrictions to take effect by the time  
294 public health officials realise an epidemic has begun. In this study we assumed  
295 a simple switch such that interactions returned to the default after the  
296 infected proportion fell back below the threshold. More realistic approaches  
297 might be to gradually ease restrictions or enact further restrictions in cases  
298 where a "2nd wave" emerges. In the similar study by Maltz and Fabricius  
299 (2016), they found a simple switch to a different proportion of local  
300 interactions led to pronounced (damped) oscillations and significant periodic  
301 outbreaks as the system was effectively moved such that it was no longer at its  
302 steady state. Further investigation in to the use of movement restrictions as a  
303 control mechanism is needed to explore the best strategies.

304 Combining mathematical analysis, using the pair approximation (Matsuda  
305 et al, 1992; Sato et al, 1994), and stochastic simulations has allowed us to  
306 explore the dynamics of our model in depth. Interestingly we found that the  
307 deterministic results from the pair approximation model provide a good  
308 'average' of the dynamics from fully-spatial stochastic simulations. The  
309 weakest 'fits' were for low values of  $R_0$ , where a proportion of simulations lead  
310 to failed epidemics, whereas the analytical model always assumes an outbreak

311 occurs. Given the problems in accurately depicting 'averages' of stochastic  
312 simulations (Juul et al, 2020), such analytic approximations may provide a  
313 useful guide.

314 We have deliberately focussed on the simplest possible epidemic model in this  
315 study, with the only two mechanisms being transmission and recovery. This  
316 has allowed us to draw clear conclusions and insight in to the behaviour of the  
317 model, but it clearly cannot and should not be used as an accurate predictive  
318 model for a particular epidemic. In an earlier study, Maltz and Fabricius  
319 (2016) considered the same model with simple demographics, finding that the  
320 infected equilibrium reduces with more local contacts, while (Webb et al,  
321 2007a) examined the impact of varying local interactions on a fully ecological  
322 model, noting the potential for disease-induced extinctions and endemic cycles  
323 of disease. Clearly, however, there are many further elements that could be  
324 considered to make the model appropriate for specific infections or systems. A  
325 standard extension for many disease models is to add an exposed  
326 compartment, separating out those that are infected from those that are also  
327 infectious (see Keeling and Rohani, 2008). It may also be instructive to  
328 consider the dynamics if immunity to infection wanes over time, since the  
329 non-spatial model would then yield an endemic equilibrium, unlike our model.  
330 If we wish to consider a disease persisting over the long-term, we should not  
331 only add demographics but also consider seasonal-forcing (Aron and Scharz,  
332 1984; Schwartz, 1985; Altizer et al, 2006). Finally, more realistic spatial and  
333 social networks would be needed for any conclusions around  
334 movement/interaction restrictions in specific circumstances to be considered,  
335 such as in recent models of Covid-19 in the UK (Ferguson et al, 2020;  
336 Kucharski et al, 2020; Firth et al, 2020). As it is, our model suggests that  
337 significant movement restrictions may be a useful strategy in tackling an  
338 epidemic.



339 **Acknowledgements**

340 LW received an Undergraduate Research Internship stipend from The School  
341 of Mathematics and Statistics at Sheffield University.

342 **References**

- 343 Altizer S, Dobson A, Hosseini P, Hudson PJ, Pascual M, Rohani P (2006)  
344 Seasonality and the dynamics of infectious disease. *Ecology Letters* 9:467-484
- 345 Anderson RM, May RM (1979) Population biology of infectious diseases: Part  
346 I. *Nature* 280:361-367
- 347 Anderson RM, May RM (1981) The population dynamics of microparasites  
348 and their invertebrate hosts. *Philosophical Transactions of the Royal Society*  
349 *of London, Series B, Biological Sciences* 291(1054):452-524
- 350 Aron JL, Scharz IB (1984) Seasonality and period-doubling bifurcations in an  
351 epidemic model. *Journal of Theoretical Biology* 110:665-679
- 352 Best A, Webb SD, White A, Boots M (2011) Host resistance and coevolution  
353 in spatially structured populations. *Proceedings of the Royal Society of*  
354 *London B: Biological Sciences* 278:2216-2222
- 355 Best A, Webb SD, Antonovics J, Boots M (2012) Local transmission processes  
356 and disease-driven host extinctions. *Theoretical Ecology* 5:211-217
- 357 Boots M, Sasaki A (1999) 'Small worlds' and the evolution of virulence:  
358 infection occurs locally and at a distance. *Proceedings of the Royal Society*  
359 *of London B: Biological Sciences* 266:1933-1938
- 360 Boots M, Sasaki A (2000) The evolutionary dynamics of local infection and  
361 global reproduction in host-parasite interactions. *Ecology Letters* 3:181-185
- 362 Débarre F, Lion S, van Baalen M, Gandon S (2012) Evolution of host  
363 life-history traits in a spatially structured host-parasite system. *The*  
364 *American Naturalist* 179:52-63

- 365 Ellner SP (2001) Pair approximation for lattice models with multiple  
366 interactions scales. *Journal of Theoretical Biology* 210:435–447
- 367 Ferguson N, Laydon D, Nedjati-Gilani, et al (2020) Report 9: Impact of  
368 non-pharmaceutical interventions (npis) to reduce covid-19 mortality and  
369 healthcare demand. Tech. rep., Imperial College London
- 370 Firth J, Hellewell J, Klepac P, Kissler S, Jucharski A, Spurgin L (2020) Using  
371 a real-world network to model localized covid-19 control strategies. *Nature*  
372 *Medicine*
- 373 Juul J, Græsboøll K, Christiansen LE, Lehmann S (2020) Fixed-time  
374 descriptive statistics underestimate extremes of epidemic curve ensembles,  
375 arXiv:2007.05035
- 376 Kamo M, Sasaki A, Boots M (2007) The role of trade-off shapes in the  
377 evolution of parasites in spatial host populations: an approximate analytical  
378 approach. *Journal of Theoretical Biology* 244:588–596
- 379 Keeling M, Rohani P (2008) *Modeling Infectious Diseases in Humans and*  
380 *Animals*. Princeton University Press
- 381 Keeling M, Rand D, Morris A (1997) Correlation models for childhood  
382 epidemics. *Proceedings of the Royal Society B: Biological Sciences*  
383 264:1149–1156
- 384 Keeling MJ (1999) The effects of local spatial structure on epidemiological  
385 invasions. *Proceedings of the Royal Society of London B: Biological Sciences*  
386 266:859–867
- 387 Kermack WO, McKendrick AG (1927) Contributions to the mathematical  
388 theory of epidemics - 1. *Proceedings of the Royal Society of London B:*  
389 *Biological Sciences* 115A:700–721
- 390 Kucharski A, Russell T, Diamon C, Liu Y, Edmunds J, Funk S, Eggo R (2020)  
391 [www.thelancet.com/infection](http://www.thelancet.com/infection) vol 20 may 2020553articleearly dynamics of

- 392 transmission and control of covid-19: a mathematical modelling study.  
393 *Lancet: Infectious Diseases* 20:553–558
- 394 Maltz A, Fabricius G (2016) Sir model with local and global infective contacts:  
395 A deterministic approach and applications. *Theoretical Population Biology*  
396 112:70–79
- 397 Matsuda H, Ogita N, Sasaki A, Sato K (1992) Statistical mechanics of  
398 population: the lattice Lotka-Volterra model. *Progress of Theoretical*  
399 *Physics* 88(6):1035–1044
- 400 Rand DA, Keeling M, Wilson HB (1995) Invasion, stability and evolution to  
401 criticality in spatially extended, artificial host-pathogen ecologies.  
402 *Proceedings of the Royal Society of London B: Biological Sciences* 259:55–63
- 403 Sato K, Matsuda H, Sasaki A (1994) Pathogen invasion and host extinction in  
404 lattice structured populations. *Journal of Mathematical Biology* 32:251–268
- 405 Schwartz IB (1985) Multiple stable recurrent outbreaks and predictability in  
406 seasonally forced nonlinear epidemic models. *Journal of Mathematical*  
407 *Biology* 21:347–361
- 408 Sharkey K (2008) Deterministic epidemiological models at the individual level.  
409 *Journal of Mathematical Biology* 57:311–331
- 410 Webb SD, Keeling MJ, Boots M (2007a) Host-parasite interactions between  
411 the local and the mean-field: how and when does spatial population  
412 structure matter? *Journal of Theoretical Biology* 249:140–152
- 413 Webb SD, Keeling MJ, Boots M (2007b) Spatially extended host-parasite  
414 interactions: The role of recovery and immunity. *Theoretical Population*  
415 *Biology* 71:251–266